CHEMISTRY
A EUROPEAN JOURNAL

Maleimido-Terminated Self-Assembled Monolayers

Yayun Wang,[a] Jun Cai,[b] Hubert Rauscher,[b] Rolf Jürgen Behm,[b] and Werner A. Goedel*[a, c, d, e]

Abstract: Four approaches have been explored for the preparation of maleimido-functionalized self-assembled monolayers (SAMs) on silicon. SAMs prepared by self-assembly of maleimido-functionalized alkyltrichlorosilanes (11-maleimido-undecyl-trichlorosilane) on oxide-covered silicon yield higher signals from maleimido functionalities in ATR-IR (attenuated total reflection IR) spectroscopy and XPS (X-ray photoelectron spectroscopy) than the other three methods. The surface composition of maleimido groups was tailored further by the formation of mixed monolayers with nonfunctionalized alkyltrichlorosilanes (decyltrichlorosilane). The order of the alkyl chains within the monolayers only slightly depends on the composition of the mixed monolayers. We utilized the maleimido-terminated SAMs to bind various nucleophilic compounds, alkylamines, alkylthiols, and thiol-tagged DNA oligonucleotides by means of conjugate addition.

Keywords: conjugate addition · maleimide · monolayers · self-assembly · silanes

Introduction

Fundamental properties of solid materials, such as adhesion, wettability, and chemical reactivity, are determined predominantly by the first layer of atoms or molecules at the surface. Surfaces can be modified at the molecular level by Langmuir–Blodgett transfer, physical adsorption, or chemisorption of monolayers to solid substrates.[1] Self-assembled monolayers (SAMs) offer one convenient route for the preparation of chemically and structurally well-defined organic monolayers. In these systems, organic molecules are covalently bound to a surface through reactive groups. This binding process is further enhanced by additional interactions between comparatively long and densely packed alkyl chains. Two types of self-assembled monolayers have been extensively studied and have shown great promise as a means of controlling surface properties: alkane thiolates on gold and alkylsilanes on silica or glass.[2] Advantages of thiols on gold are their ease of preparation and the high order of the obtained monolayers. On the other hand, alkylsilanes are advantageous because the monolayers are comparatively stable (chemically and thermally) and can be formed on various inorganic oxides, including transparent dielectrics.[3]

Furthermore, desired functionalities can be introduced by chemical modification of the terminal groups of the SAMs, for example by nucleophilic substitution,[4] hydrogenation,[5,6] and carbonyl reaction.[7,8] While a variety of useful functional groups, such as amine[4,9,10] and hydroxy,[11–13] have been well-studied previously, maleimido-functionalized self-assembled monolayers have drawn increasing attention recently. Maleimido groups are capable of reacting with thiol or amino functionalities (Figure 1) under mild conditions and thus have appealing properties, especially for the immobilization of biomolecules, such as DNA-oligonucleotides or proteins. A single-step preparation of maleimido-terminated monolayers on gold surfaces was reported recently,[14,15] Fur-

[a] Y. Wang, Prof. Dr. W. A. Goedel
Organic and Macromolecular Chemistry, OCIII
University of Ulm, 89069 Ulm (Germany)
E-mail: werner.goedel@chemie.tu-chemnitz.de

[b] Dr. J. Cai, Dr. H. Rauscher, Prof. Dr. R. J. Behm
Surface Chemistry and Catalysis
University of Ulm, 89069 Ulm (Germany)

[c] Prof. Dr. W. A. Goedel
Material Science & Catalysis, ACII
University of Ulm (Germany)

[d] Prof. Dr. W. A. Goedel
Polymer Physics, Polymer Research
BASF-Aktiengesellschaft (Germany)

[e] Prof. Dr. W. A. Goedel
Physical Chemistry, Chemnitz University of Technology
Strasse der Nationen 62, 09111 Chemnitz (Germany)
Fax: (+49) 371-531-1371

Supporting information for this article is available on the WWW under http://www.chemeurj.org/ or from the author.

DOI: 10.1002/chem.200400896

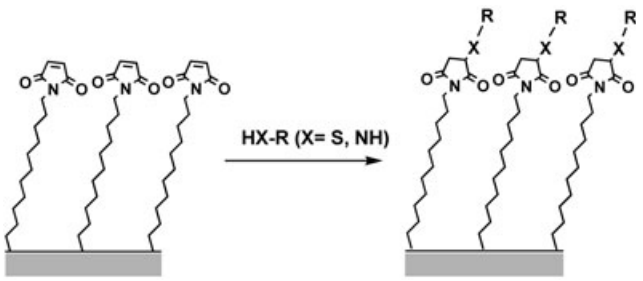

Figure 1. General sketch of the use of maleimido-terminated monolayers to bind thiols or amines to a surface by means of conjugate addition.

thermore, the monolayers were successfully utilized to immobilize various peptides and carbohydrates,[14,16,17] If, on the other hand, maleimido-terminated monolayers on glass or oxide-covered surfaces are desired, the currently used preparation involves a cascade of surface reactions, namely, complex preparation of silane-based SAMs with nucleophilic functionalities and a subsequent reaction with a heterocrosslinker bearing the maleimido moiety.[18–20] The implementation of surface reactions has the disadvantage that their completion is often hindered by interfacial effects, such as steric hindrance.[9] In addition, it is impossible to purify unreacted groups or surface-bound side products from the desired functionalities. Therefore, it is desirable to decrease the number of surface reactions involved or, ideally, to prepare the monolayers in a single-step surface reaction, as has already been demonstrated in the case of thiol monolayers on gold.[14–17]

Herein, we develop three approaches for the preparation of maleimido-functionalized SAMs (Scheme 1, methods 2–4) and compare them with the conventional approach adopted from reference [20] (Scheme 1, method 1). The properties of such monolayers are tailored even further by deposition from solutions of trichlorosilane mixtures. In addition, we utilize the maleimido-functionalized surface to bind various nucleophilic reagents and thiol-tagged DNA oligonucleotides.

Results and Discussion

The established preparation of maleimido-functionalized monolayers,[20] as shown in Scheme 1 method 1, involves a cascade of surface reactions: nucleophilic substitution of a heterocrosslinker-bearing maleimido group (for example, SSMCC sulfosuccinimidyl 4-(*N*-maleimidomethyl)cyclohexane-1-carboxylate) by amino-terminated SAMs, which are obtained by formation of bromo-terminated SAMs on oxide-covered silicon, nucleophilic displacement of bromine by azide, and subsequent reduction.[4] Three new routes, as shown in Scheme 1 methods 2, 3, and 4 have been designed. Method 2 utilizes the surface reaction between bromo-terminated SAMs on silicon and a protected maleimide (3,6-endoxo-Δ^4-tetrahydrophthalimide, PM) followed by deprotection. In method 3, the surface immobilization is implemented by hydrosilylation of a maleimido-functionalized olefin (11-maleimido-undecene, MU) on a hydrogen-terminated silicon surface. In method 4, maleimido-functionalized trichlorosilane is reacted with oxide-covered silicon.

As shown in Scheme 2, the maleimido-terminated trichlorosilane (ω-maleimido-undecyltrichlorosilane, MUTS) necessary for method 4 is synthesized from commercial starting materials by a novel four-step route. Two compounds in the route, PM and MU, are used in method 2 and 3, respectively.

In the following, we 1) present the details of the synthesis of the individual compounds; 2) compare the properties of maleimido-terminated surfaces obtained by the various routes; 3) explore the preparation of mixed monolayers comprising maleimido- and methyl-terminated trichlorosilanes; 4) examine the reactions of maleimido-modified monolayers from method 4 with a variety of nucleophiles and thiol-tagged DNA oligonucleotides.

Synthesis of the necessary building blocks for the preparation of maleimido monolayers for methods 2, 3, and 4: The classic method to produce *N*-alkylated maleimide derivatives involves a condensation reaction between an appropriately substituted amine and maleic anhydride followed by acid-promoted dehydration and ring closure. However, the ring closure is often inefficient and thus only poor yields of the desired maleimide derivatives are obtained. A newly developed approach[21] utilizes nucleophilic substitution of alkyl bromide with a maleimide (PM) protected with furan by a Diels–Adler reaction[22,23] and subsequent deprotection to afford a high yield of *N*-substituted maleimide. We used ω-bromoundecene and PM as starting materials (see Scheme 2b), and obtained a high yield (80%) of 11-maleimido-undecene (MU), which is comparable with the yields reported. PM and MU are used for method 2 and method 3, respectively.

We subjected the intermediate MU to hydrosilylation with $HSiCl_3$ and obtained the desired maleimdo-functionalized trichlorosilane (MUTS), which is then used to prepare self-assembled monolayers in method 4.

Characterization of the self-assembled monolayers: The maleimido-terminated monolayers on the surface of a silicon crystal, prepared by the four methods illustrated in Scheme 1, were characterized by attenuated total reflection infrared (ATR-IR) spectroscopy, X-ray photoelectron spectroscopy (XPS), atomic force microscopy (AFM), and ellipsometry.

In the IR spectra, the cyclic imide carbonyl groups exhibit two bands in the region between 1700 and 1800 cm^{-1}. One band is located between 1800 and 1740 cm^{-1} (symmetric stretch) and a more intense band between 1740 and 1700 cm^{-1} (antisymmetric stretch).[24] As Figure 2 shows, the absorption band of the carbonyl antisymmetric stretch at about 1705 cm^{-1} is present in all the maleimido-terminated monolayers obtained by the four methods, whereas the symmetric stretching absorption band at 1770 cm^{-1} shows up

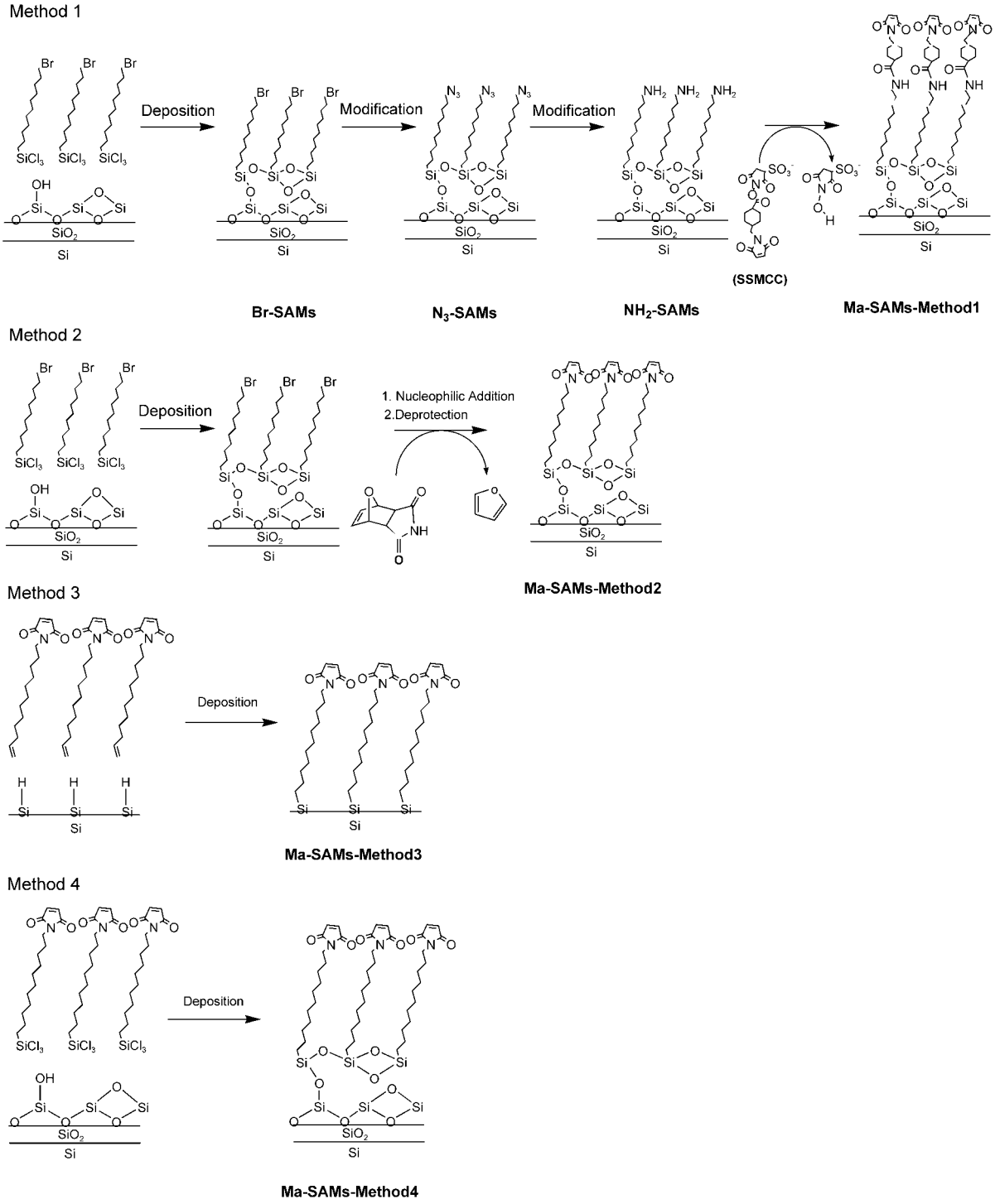

Scheme 1. The four methods used to synthesize the maleimido-terminated monolayers used here.

above the noise level only in the monolayers obtained by method 4. The monolayers obtained from method 4 gives rise to an absorbance at about 1706 cm^{-1}, which is significantly greater than that observed in the case of the other methods.

The elemental compositions measured by XPS of the surfaces obtained by using methods 1–4 are given in Table 1. The starting Br-SAMs in the conventional method, method 1, show a significant Br 3d signal, which dramatically decreased after the nucleophilic substitution by the azide. The introduction of azide groups was indicated by the simultaneous appearance of N 1s signals. The reduction of the azide groups to amino groups gives rise to a decrease of the nitrogen signal. Maleimido groups, introduced by nucleophilic substitution of the hetero-crosslinker (SSMCC) by the

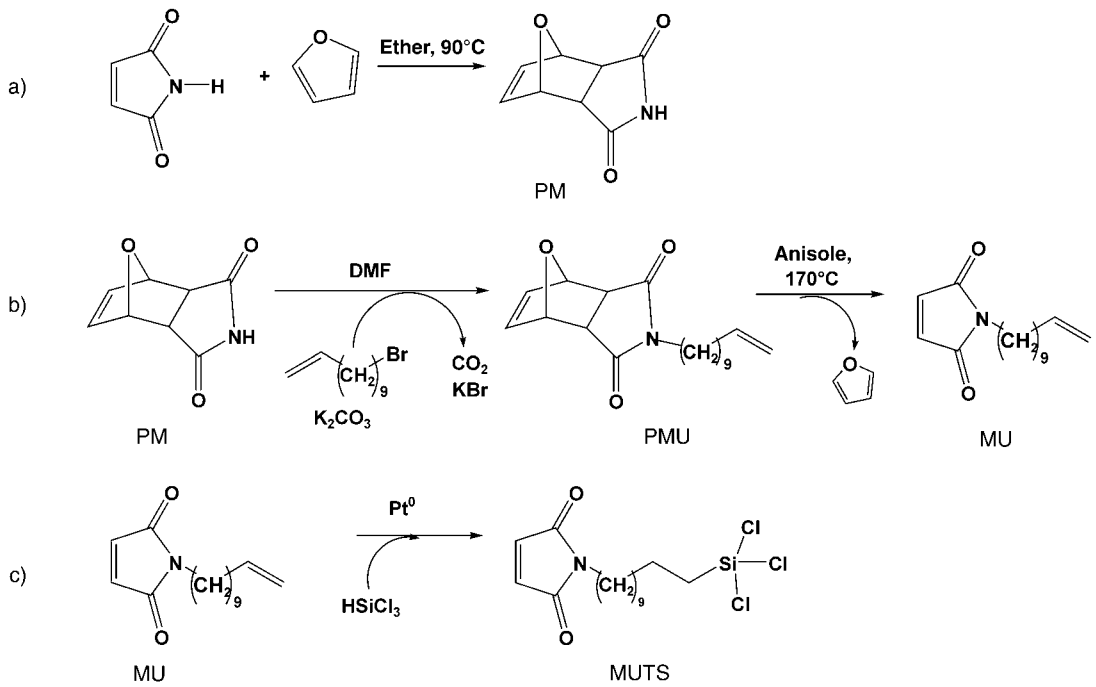

Scheme 2. Synthesis of the protected maleimide (PM) used in method 2, of 11-maleimido-1-undecene (MU) used in method 3, and of 11-maleimido-undecyltrichlorosilane (MUTS) used in method 4.

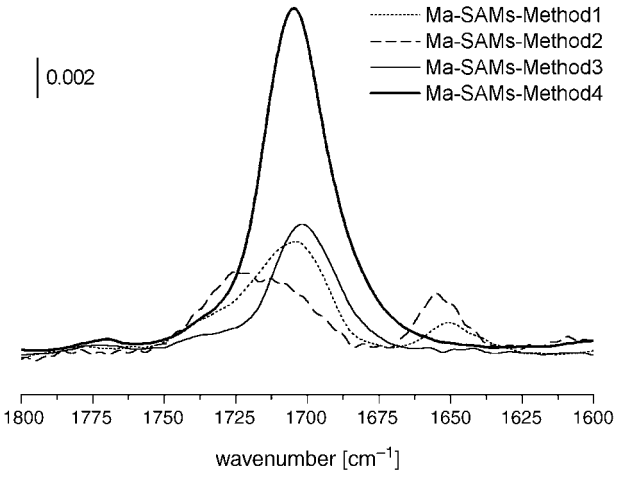

Figure 2. ATR-IR spectra of maleimido-terminated monolayers prepared by the four methods shown in Scheme 1.

Table 1. XPS elemental composition of SAMs prepared by the four methods

SAMs type[a]	Elemental composition [atom %]		
	Br 3d	N 1s	C 1s
Br-SAMs	2.3	[b]	35.8
N_3-SAMs	0.2	5.2	33.2
NH_2-SAMs	0.1	2.0	37.7
Ma-SAMs-Method1	0.1	3.4	50.4
Ma-SAMs-Method2	0.6	1.8	40.5
Ma-SAMs-Method3	[b]	2.1	34.0
Ma-SAMs-Method4	[b]	3.1	38.6

[a] Ma refers to the maleimido-terminated SAMs. [b] No peak visible.

amino-terminated SAMs, give rise to an increase of the N 1s signal. The two-step route of method 2, the surface nucleophilic substitution of Br-SAMs by the deprotonated protected maleimide (PM), also involves a reduction in the Br 3d signal and the simultaneous appearance of N 1s signals. It is worth nothing that in both methods, the Br 3d signal does not vanish completely and thus indicates incomplete conversion in the surface reactions.

High-resolution XPS of the monolayers obtained by using methods 1–4 in the N 1s region are shown in Figure 3. The N 1s peak of the monolayers obtained by using method 1 is broader and has a higher intensity than those obtained from

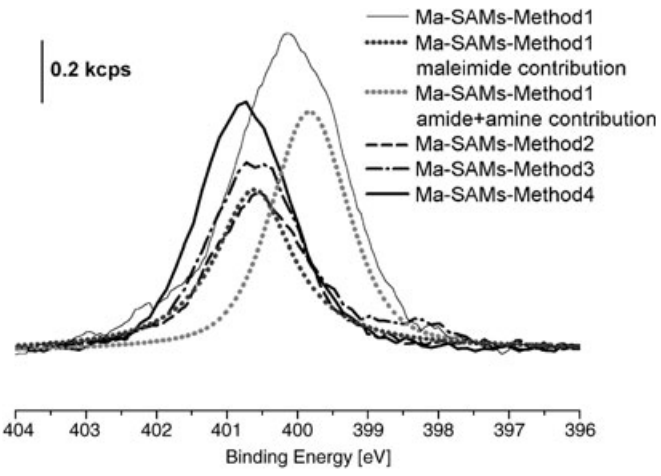

Figure 3. High-resolution XPS in the N 1s region of maleimido-terminated monolayers prepared by the four methods.

the other methods. This is attributed to the fact that the peak is composed of contributions assigned to the maleimide, the amide formed in the last reaction step, and amines that were not converted. A deconvolution of the broad peak into the above-mentioned contributions is shown by the two dotted lines.

In principle, the signal intensities in the ATR-IR spectra and X-ray photoelectron spectra might be regarded as an indicator of the amount of maleimido functionalities bound to the surface. However, the signal intensities are influenced by additional factors: in IR spectroscopy, the signal is influenced by the relative orientation of the chromophores, whereas in XPS the signal intensity is decreased if groups are buried within the sample. Although the interpretations of the results from both methods are not straightforward in terms of surface concentrations, it is worth pointing out that the intensities of the signals assigned to the maleimido group increase from method 1 to method 4 both in the IR spectra and the X-ray photoelectron spectra.

Ellipsometry indicates that for all four methods the obtained thickness is largely in agreement with the formation of monolayers. Methods 2–4 yield a thickness comparable to that of the methyl-terminated monolayers prepared from decyltrichlorosilane (DTS). Method 1 affords a significantly greater thickness, which can be attributed to the binding of the hetero-crosslinker (data given in the Supporting Information).

The use of very carefully cleaned surfaces and precisely controlled deposition conditions has shown that ultrasmooth SAMs can be prepared with a root mean square (rms) roughness of <1.0 Å.[25] Less optimal conditions would probably lead to imperfect monolayers with a higher roughness. Therefore, it is of interest to use atomic force microscopy to investigate the roughness of the surfaces involved here. In our case, the two surfaces treated with trichlorosilanes (the bromo-terminated SAMs after step 1 in method 1 and the maleimido-terminated SAMs in method 4) have a rms roughness value of 2.8 and 2.0 Å, respectively. These values are similar to that of a plain silicon substrate (rms roughness $=$ 2.2 Å). It appears that each step in method 1 introduces additional roughness: the root mean square roughness increases from 2.8 to 5.0 Å from Br-SAMs to Ma-SAMs. Method 2 and method 3 produce an even rougher surface than method 1 (rms roughness $=$ 6.4 and 9.2 Å, respectively). The AFM images of the plain silicon substrates and the silane-treated surfaces are given in the Supporting Information.

From an analysis of the above results, we conclude that method 4 is more suitable for the generation of monolayers bearing maleimido groups than the other three routes investigated here. Therefore, we utilized this route in further investigations.

Preparation of mixed monolayers: One great advantage of preparing SAMs from trichlorosilane is that one can easily tailor surface functionalization by mixing functionalized and nonfunctionalized trichlorosilanes.[26]

In this work, we tuned the properties of the monolayers by mixing maleimido-functionalized silanes (MUTS) with methyl-functionalized silanes (decyltrichlorosilane, DTS). By varying the concentration ratio of MUTS and DTS (0:1, 1:2, 2:1, 1:0) in the original deposition solution, we influenced the composition of the monolayers in a continuous manner: the absorption intensity at about 1706 cm^{-1}, assigned to the carbonyl antisymmetric stretch vibration of the maleimido carbonyl groups, increased with increasing molar ratio of MUTS in the deposition solution (see Figure 4a and Figure 5).

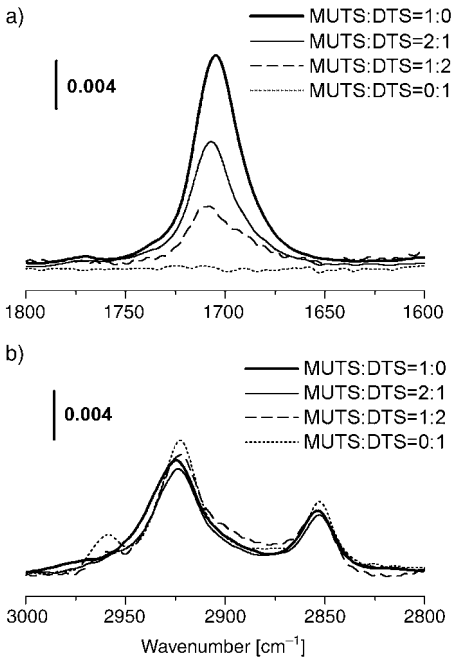

Figure 4. ATR-IR absorbance spectra of mixed SAMs prepared from deposition solutions with different molar ratio of MUTS and DTS, a) in the carbonyl region, b) in the methylene region.

The frequencies of the symmetric and antisymmetric methylene stretching vibrations are sensitive to the conformational order of the alkyl chain in the self-assembled monolayers. The value of the antisymmetric vibration at 2918–2919 cm^{-1} corresponds to all-*trans* alkyl chain conformations and a value of 2928 cm^{-1} to liquid-like disordered chains.[27] It has been shown that the order of the SAMs decreases with decreasing chain length. Methyl-terminated SAMs with a chain length between C10 and C11 have a CH_2-antisymmetric absorption at 2293–2294 cm^{-1},[28,29] suggesting a relatively disordered monolayer. In Figure 4b and Figure 5, variation of the composition of the mixed monolayers (from maleimido-SAMs to methyl-terminated SAMs) gave rise to a minor shift of the methylene antisymmetric stretch absorption (from 2924.5 to 2923.0 cm^{-1}). We thus estimate that the degree of ordering of the alkyl chain in the maleimido-terminated monolayers and mixed monolayers is only slightly dependent on the composition.

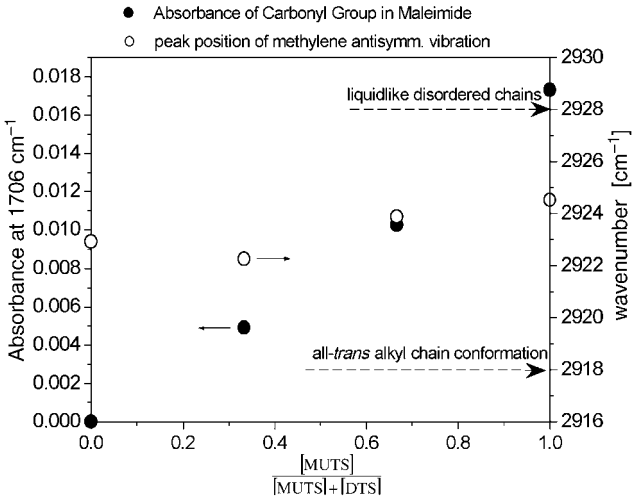

Figure 5. ATR-IR absorption intensity of the carbonyl peak and peak position of the CH_2-antisymmetric stretch vibration as a function of the molar fraction of MUTS in the deposition solution ([MUTS]/([MUTS]+[DTS])).

The mixed monolayers were further investigated by XPS. The high-resolution C 1s spectrum of the maleimido SAMs prepared by method 4 (Figure 6a) presents three components at binding energies of 284.5 eV (67.8%), 285.5 eV (21.6%), and 288.4 eV (10.6%).[30] The dominant peak at 284.5 eV is assigned to the saturated hydrocarbon part of the monolayers.[31,32] The other two components at higher binding energies primarily originate from the carbon atoms involved in various bonding arrangements with oxygen and nitrogen (C–N, N–C=O). Additionally, the carbon atoms within the conjugated system of the maleimide ring are also supposed to have a higher binding energy as a result of conjugation.

The high-resolution C 1s and N 1s spectra of the mixed monolayers are shown in Figure 6b and c, respectively. The corresponding integral intensities are presented in Table 2 and are plotted in Figure 7 versus the molar fraction of maleimido-terminated trichlorosilane in the deposition solution. The intensities of the peaks corresponding to the nitrogen (400.7 eV) and to the carbon atoms within or connected to the maleimido group (285.5 eV and 288.4 eV) increase roughly linearly with the composition of the deposition solution. On the other hand, the signal corresponding to the aliphatic carbons (284.5 eV) seems to be almost unaffected by the mixing ratio.

Figure 8 shows a plot of the advancing and receding contact angles of water on the mixed monolayers versus the molar fraction of MUTS in the deposition solution ([MUTS]/([MUTS]+[DTS])). The contact angles decrease with increasing fraction of maleimido-functionalized alkyltrichlorosilanes in the deposition solution, which could be explained by the increasing maleimido moieties deposited on the surface, which have a higher hydrophilicity than methyl groups. An increasing hysteresis was observed when more maleimido moieties—polar groups—were deposited

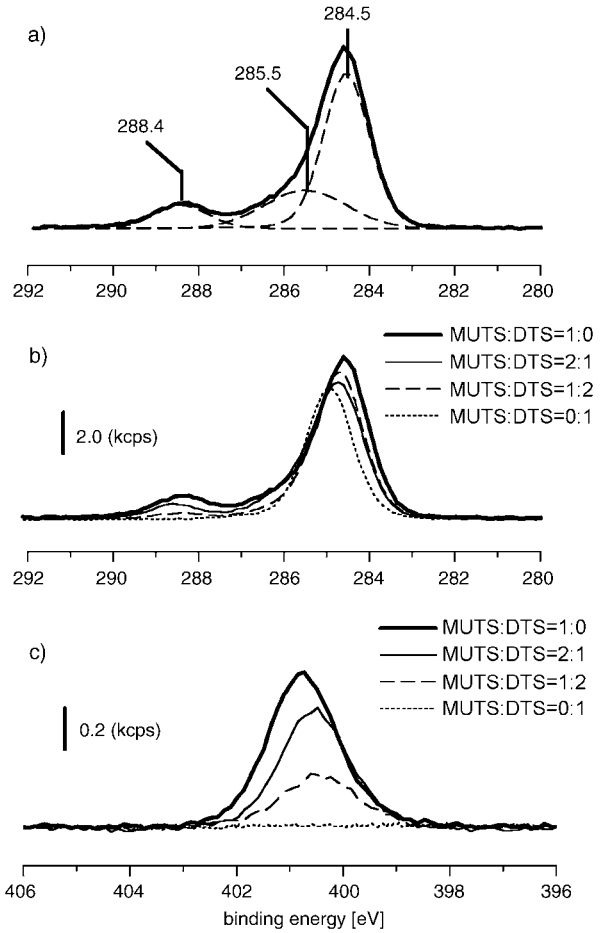

Figure 6. a) Analysis of high-resolution C 1s spectra of maleimido-terminated SAMs obtained with method 4 by fitting three Gauss–Lorentz peaks. b) High-resolution XPS in the C 1s region of mixed monolayers composed of maleimido and methyl end groups. c) High-resolution XPS in the N 1s region of mixed monolayers composed of maleimido and methyl end groups.

Table 2. XPS elemental composition of mixed monolayers composed of maleimido and methyl end groups.[a]

Mixed monolayers	Elemental composition [atom%]		C 1s area[b]	C 1s area[b]	C 1s area[b]
	N 1s	C 1s	at 284.5 eV	at 285.5 eV	at 288.4 eV
Ma:CH_3 = 1:0	3.1	38.6	67.8	21.6	10.6
Ma:CH_3 = 2:1	2.4	38.1	74.9	16.6	8.5
Ma:CH_3 = 1:2	1.2	36.3	85.4	11.4	3.2
Ma:CH_3 = 0:1	0.0	30.8	97.2	2.8[c]	[d]

[a] Ma refers to the maleimido-terminated SAMs. [b] Atom% of signal. [c] Peak at 286.5 eV. [d] No peak visible.

on the surface, which is in accordance with examples in the literature.[33]

All parameters measured above that, in principle, are sensitive to the surface concentration of the maleimido groups (intensity of the IR peak at 1706 cm^{-1}, N 1s and C 1s XPS signal, water contact angle) depend linearly on the molar fraction of the maleimido functionalized silanes in the deposition solution (Figure 5, Figure 7, Figure 8). Furthermore,

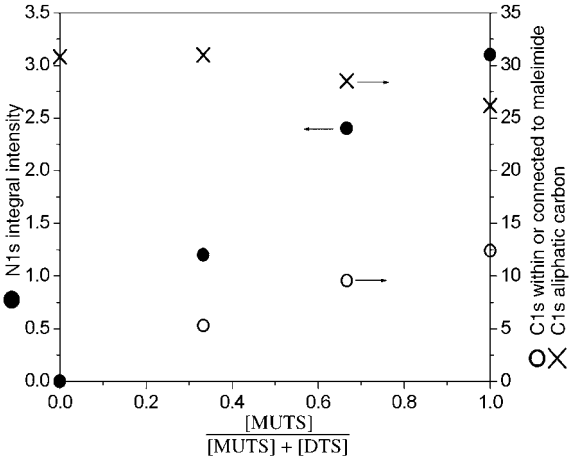

Figure 7. Integral intensities of the N 1s signal (400.7 eV) and of the contributions to the C 1s signals from carbon atoms within or connected to the maleimido group (285.5 eV and 288.4 eV) and from aliphatic hydrocarbons of the alkyl chain (284.5 eV) in XPS as a function of the molar fraction of MUTS in the deposition solution ([MUTS]/([MUTS]+[DTS])).

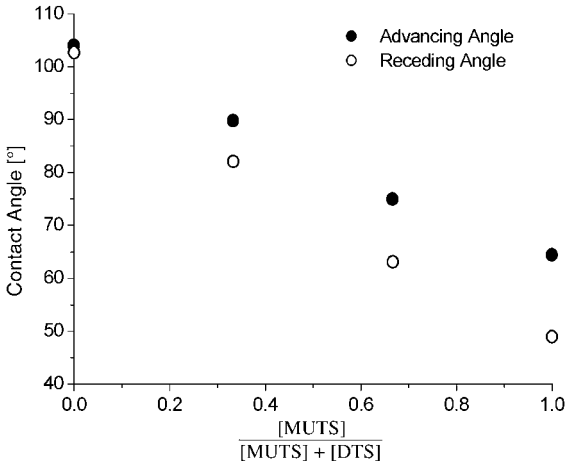

Figure 8. Water contact angles of mixed SAMs as a function of the molar fraction of MUTS in the deposition solution ([MUTS]/([MUTS]+[DTS])).

IR spectroscopy of the methylene groups indicates only insignificant changes in the packing order of the alkyl chains. In combination, these observations can be interpreted as nonpreferential uniform binding of both compounds from solution.

Reactivity of the maleimido-terminated SAMs: To explore the reactivity of the maleimido moieties on the surface, we exposed the maleimido-terminated SAMs produced by method 4 to various nucleophilic compounds. Based on similar reactions occurring in solution,[34,35] we expected the surface reactions shown in Scheme 3.

The conjugate addition of thiol was investigated by exposure to decylthiol and octadecylthiol under mild conditions (55 °C in ethanol). In both cases, the absorption in the region of methylene stretching increases (Figure 9 and Figure 10, a and b). The difference spectra (Figure 9 and Figure 10, c) of maleimido-SAMs before and after reaction with the alkylthiols show the binding of additional alkyl chains to the underlying SAMs. In the case of decylthiol, the difference spectrum shows a weak signal whereas that of octadecylthiol shows a strong peak. In the maleimide ring, there is conjugation between the carbonyl groups, the double bond, and the N atom. The addition of the double bond might influence the carbonyl absorption position in the IR spectrum. However, no systematic shift was observed in our experiments. On the other hand, in previous research carried out on similar reactions in homogeneous solutions, no systematic shifts were reported either.[21,36]

The monolayers were also allowed to react with aliphatic amines, isoindole, and thioacetamide. All of them were labeled with a cyano group as IR spectroscopic marker. As Figure 11 shows, all spectra of the monolayers after exposure to the nucleophiles show a peak in the region between 2300 and 2100 cm^{-1} that can be assigned to the cyano group. We thus conclude that these surface reactions also proceed as shown in Scheme 3.

In further experiments, silicon surfaces that were covered with maleimido-terminated monolayers were immersed in aqueous buffer solutions of thiol-tagged DNA oligonucleotides, thoroughly rinsed, and characterized with XPS (Figure 12). Before the exposure to DNA oligonucleotides (dashed line), the X-ray photoelectron spectra showed a peak in the region of N 1s (at 400.7 eV), which is assigned to the maleimide. However, the spectra showed no detectable signal in the P 2p region. After the exposure, the N 1s peak increased in intensity (from 3.1 to 6.5) and a peak appeared in the P 2p region at 133.9 eV. Because the backbone of the DNA molecules comprises phosphate moieties, we conclude that the immobilization of DNA oligonucleotides occurred.

Conclusion

Maleimido-functionalized alkyl trichlorosilanes can be prepared with moderate synthetic effort. They can be used for the generation of maleimido-terminated self-assembled monolayers in a single step and give rise to higher surface concentrations than those of monolayers prepared by a previously published multistep procedure. The properties of the monolayers can be tuned by mixing with methyl-functionalized alkyltrichlorosilanes. The maleimido groups are efficient in covalently binding nucleophilic heterocycles, alkylthiols, amines, and thiol-tagged DNA oligonucleotides.

Experimental Section

Self-assembled monolayers were prepared on silicon surfaces. Si ATR crystals (Korth GmbH, Berlin, parallelipeds with an angle of 45°, 72 mm × 12 mm × 6 mm) were used for IR spectroscopy and contact-angle

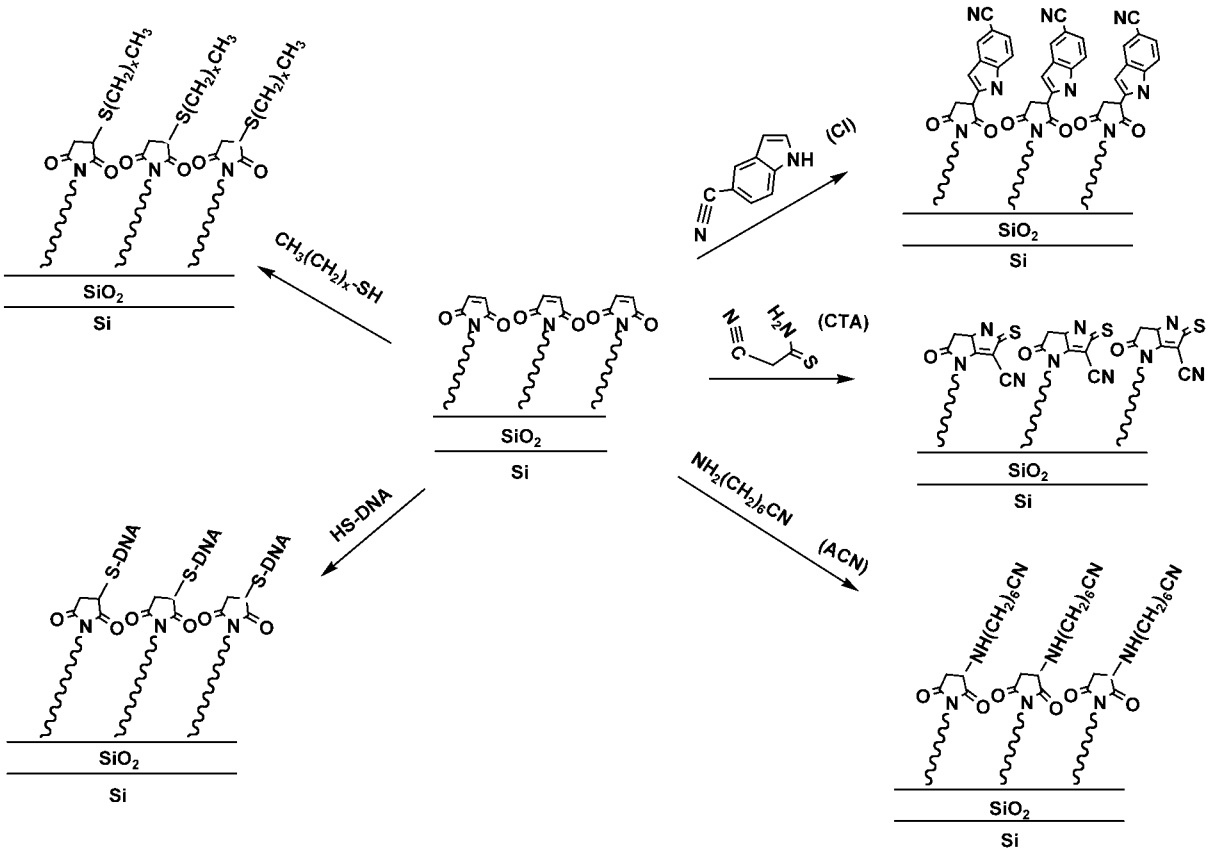

Scheme 3. Schematic representation of reactions between maleimido-terminated SAMs prepared by method 4 with various nucleophiles.

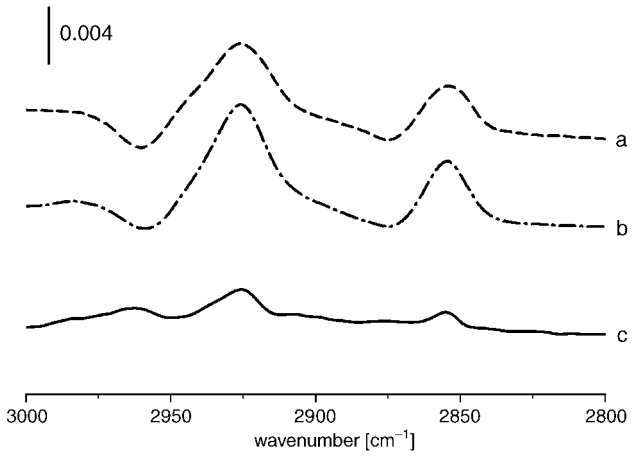

Figure 9. ATR-IR spectra of maleimido-SAMs prepared by method 4 before and after reaction with decylthiol: a) maleimido-SAMs, b) maleimido-SAMs + thiol, c) difference between spectra b and a.

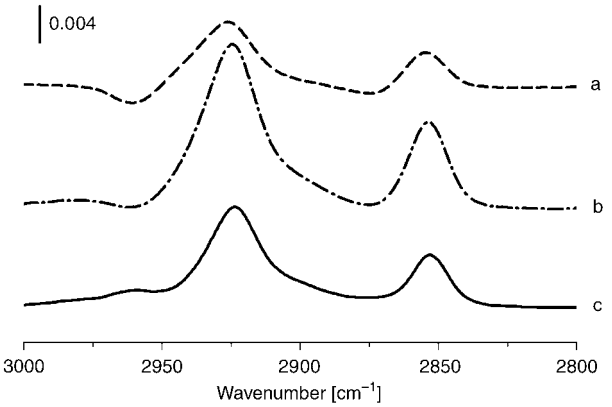

Figure 10. ATR-IR spectra of maleimido-SAMs prepared by method 4 before and after reaction with octadecylthiol: a) maleimido-SAMs, b) maleimido-SAMs + thiol, c) difference between spectra b and a.

measurements. Si wafers (Crystec GmbH, Berlin, orientation 100, *p* type, >1 ohm cm^{-1}) were used for XPS (size: 10 mm × 5 mm), AFM (size: 10 mm × 10 mm), and ellipsometry measurements (size: 10 mm × 10 mm).

11-Bromo-1-undecene (BU):[37] 10-Undecen-1-ol (85 g, 0.5 mol) was dissolved in a mixture of dry toluene (140 mL, dried through aluminum oxide, neutral) and pyridine (27 mL). The solution was cooled to −10 °C, and kept at −5 °C to −10 °C while a solution of phosphorus tribromide (54.2 g, 0.2 mol) in dry toluene (140 mL) was added over a period of 2 h. The reaction mixture was allowed to warm to room temperature, and was then heated to 100 °C for 2 h with stirring. After the mixture was allowed to cool to room temperature, the supernatant liquid layer was decanted from the yellow precipitate. The precipitate was washed with a small amount of toluene. The toluene used for washing was added to the decanted liquid, and the toluene was removed by rotary evaporation under reduced pressure. The oily residue was further dried at 0.13–0.40 mbar, 25 °C. Afterwards, it was diluted with an equal volume of ether. This mixture was washed (water, saturated sodium bicarbonate, saturated sodium chloride), dried over sodium sulfate, and distilled. A yield

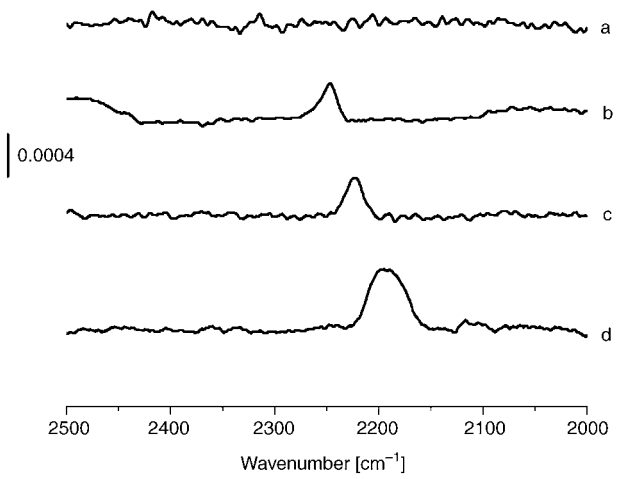

Figure 11. ATR-IR spectra of maleimido-SAMs prepared by method 4 before and after reaction with nucleophiles bearing a nitrile group as spectroscopic marker: a) maleimido-SAMs before reaction, b) maleimido-SAMs + aminocapronitrile (ACN), c) maleimido-SAMs + 5-cyanoindole (CI), d) maleimido-SAMs + 2-cyano-thioacetamide (CTA).

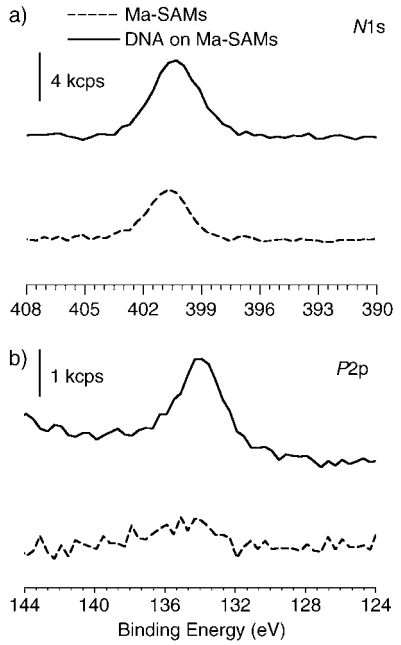

Figure 12. XPS spectra of maleimido-terminated SAMs (-----) and DNA-immobilized surface (——) in the region of a) N 1s, and b) P 2p.

of 83.77 g (71.9 %) of colorless 11-bromo-1-undecene was obtained. ^{1}H NMR (400 MHz, $CDCl_3$, 25 °C, TMS): δ = 1.14–1.50 (m, 12H), 1.86 (m, 2H), 2.06 (m, 2H), 3.41 (t, J = 7 Hz, 2H), 4.88–5.02 (m, 2H), 5.80–5.92 ppm (m, 1H); ^{13}C NMR ([D_8]THF): δ = 139.14, 114.14, 33.93, 33.78, 32.84, 29.37, 29.07, 28.91, 28.75, 28.17 ppm; MS-CI (100 eV): m/z (%): 235 (29.6) $[M+2]^+$, 233 (28.5) $[M]^+$, 111 (38.4), 97 (100), 85 (32.3), 83 (82.8), 71 (39.9), 69 (31.4).

Protected maleimide (PM): *exo* isomers of 3,6-endoxo-Δ^4-tetrahydrophthalimide:[22] Maleimide (0.71 g, 7.31 mmol) was dissolved in fifty times its weight of diethyl ether (50 mL) and 50 % excess of furan (0.8 mL, 10.9 mmol). The reaction solution was heated in an autoclave for 10 h at 90 °C. The white crystalline product that separated after cooling to 4 °C was recrystallized with ethyl acetate to yield the product (0.25 g; 20.7 %). ^{1}H NMR (400 MHz, $CDCl_3$, 25 °C, TMS): δ = 2.91 (s, 2H), 5.34 (s, 2H), 6.54 (s, 2H), 7.90 ppm (s, 1H); ^{13}C NMR ([D_8]THF): δ = 176.64; 136.50; 80.97; 48.79 ppm; MS-CI (100 eV): m/z (%): 168 (1.6) $[M+2]^+$, 167 (1.4) $[M+1]^+$, 166 (14.3) $[M]^+$, 126 (22.7), 98 (100), 69 (41.67).

Protected maleimido-undecene (PMU): 11-(3,6-endoxo-Δ^4-tetrahydrophthalimide)undecene:[21] In an oven-dried (at 200 °C for 12 h, closed by a stopper and subsequently cooled to room temperature) round-bottom flask, PM (0.131 g, 0.8 mmol) and BU (0.2 mL, 0.8 mmol) were dissolved in anhydrous DMF (8 mL, dried over 4 Å molecular sieve) along with K_2CO_3 (0.55 g, 5 equiv). The entire reaction mixture was stirred under N_2 at 55 °C for 2.5 h. The entire reaction mixture was diluted with ethyl acetate (150 mL), washed (water, saturated sodium bicarbonate solution), and dried over Na_2SO_4. The ethyl acetate was removed at reduced pressure, and the residue was purified by column chromatography ($CHCl_3$/silica) to yield the pure product (0.2 mL; 80 %). ^{1}H NMR (400 MHz, $CDCl_3$, 25 °C, TMS): δ = 1.14–1.50 (m, 12H), 1.56 (m, 2H), 2.04 (m, 2H), 2.84 (s, 2H), 3.50 (t, J = 7 Hz, 2H), 4.88–5.02 (m, 2H), 5.28 (s, 2H), 5.80–5.92 (m, 1H), 6.52 ppm (s, 2H); ^{13}C NMR ($CDCl_3$): δ = 176.27; 139.22; 136.54; 114.09; 80.90; 47.34; 39.03; 33.78; 29.37; 29.34; 29.07; 28.90; 27.58; 26.65 ppm; MS-CI (100 eV): m/z (%): 332 (1.0) $[M]^+$, 278 (18.0), 250 (100), 248 (19.3).

11-Maleimido-undecene (MU): 1-undecylenyl-1*H*-pyrrole-2,5-dione: A mixture of PMU (0.2 mL, $\approx$0.5 mmol) and anisole (2 mL) was stirred under reflux (170 °C) for 2 h followed by removal of the anisole by Kugelrohr distillation (75 °C, 2.5×10^{-2} mbar) to afford the pure product. Yield: 0.165 g (100 %); ^{1}H NMR (400 MHz, $CDCl_3$, 25 °C, TMS): δ = 1.14–1.50 (m, 12H), 1.59 (m, 2H), 2.04 (m, 2H), 3.52 (t, J = 8 Hz, 2H), 4.88–5.02 (m, 2H), 5.80–5.92 (m, 1H), 6.69 ppm (s, 2H); ^{13}C NMR ($CDCl_3$): δ = 170.87, 139.19, 134.02, 114.11, 55.12, 37.93, 33.77, 29.39, 29.34, 29.08, 28.89, 28.52, 26.72 ppm; MS-CI (100 eV): m/z (%): 251 (43.4) $[M+2]^+$, 250 (100) $[M+1]^+$, 249 (59.2) $[M]^+$, 248 (35.2), 194 (30.0), 180 (24.1), 166 (20.1).

Catalyst for hydrosilylation: dicyclopentadienylplatinum(II) chloride [Cp_2PtCl_2]: Method adopted from reference [38]: hydrated chloroplatinic acid (0.69 g, 1.33 mmol) was dissolved in glacial acetic acid (1.5 mL) in a 25-mL flask. The solution was diluted with water (2.5 mL) and slowly heated to 70 °C. Dicyclopentadiene (0.5 mL, 3.70 mmol) was then added to the reaction vessel, and the mixture was stirred vigorously for 24 h at this temperature. The crude product precipitated, was collected by filtration, then redissolved in THF, decolorized by charcoal, and finally recrystallized from THF to yield the pure product (0.25 g; 59 %; m.p. 218 °C). The structure was verified by ^{1}H NMR (400 MHz, $CDCl_3$, 25 °C, TMS): δ = 1.84 (m, 1H), 2.16 (m, 2H), 2.35 (m, 1H), 2.86 (m, 2H), 3.65 (m, 2H), 5.53 (t, J = 36 Hz, 1H), 6.07 (t, J = 40 Hz, 1H), 6.47 (t, J = 32 Hz, 1H), 6.85 ppm (t, J = 40 Hz, 1H); ^{13}C NMR ($CDCl_3$): δ = 116.18, 105.31, 100.31, 97.42, 60.05, 56.14, 55.38, 43.67, 43.39, 33.69 ppm; MS-CI (100 eV): m/z (%): 399 (4.2) $[M+1]^+$, 398 (6.9) $[M]^+$, 365 (45.5), 364 (41.7), 363 (89.6), 362 (92.1), 361 (100).

11-Bromo-undecyl-trichlorosilane (BUTS) and 11-maleimido-undecyltrichlorosilane (MUTS); hydrosilylation of BU and MU: BU (1 mL, 431 mmol), $HSiCl_3$ (5 mL, 49.5 mmol), and the catalyst [Cp_2PtCl_2] (10 mg, 0.018 mmol) were placed in a 25-mL three-neck-flask and refluxed at 40 °C for 10–16 h under an Ar atmosphere. The disappearance of the olefinic protons was monitored with ^{1}H NMR spectroscopy. $HSiCl_3$ was distilled off, and the BUTS product was isolated by Kugelrohr distillation (170 °C–180 °C, 3×10^{-1} mbar). ^{1}H NMR (400 MHz, $CDCl_3$, 25 °C, TMS): δ = 1.14–1.50 (m, 16H), 1.59 (m, 2H), 1.87 (m, 2H), 3.41 ppm (t, J = 7 Hz, 2H); ^{13}C NMR ($CDCl_3$): δ = 33.93, 32.84, 31.78, 29.44, 29.37, 29.29, 28.98, 28.75, 28.17, 24.33, 22.25 ppm; MS-CI (100 eV): m/z (%): 369 (6.7) $[M+2]^+$, 367 (11.9) $[M]^+$, 365 (9.4), 291 (34.1), 289 (100), 287 (90.2), 235 (23.8), 231 (24.4), 219 (21.4), 113 (25.5), 99 (31.7), 85 (61.0), 71 (67.7).

The hydrosilylation conditions for MU were similar to those of BU: MU (0.2 mL, 0.6 mmol) was allowed to react with $HSiCl_3$ (0.3 mL, 2.7 mmol) and [Cp_2PtCl_2] (2×10^{-4} mg). Samples were extracted at regular intervals, and the reaction was monitored by ^{1}H NMR spectroscopy. $HSiCl_3$ was removed by distillation. ^{1}H NMR (400 MHz, $CDCl_3$, 25 °C, TMS): δ = 1.28–1.53 (m, 16H), 1.66 (m, 4H), 3.52 (t, J = 6.5 Hz, 2H), 6.69 ppm (s,

2H); ^{13}C NMR ($CDCl_3$): δ = 170.89; 134.02; 37.95; 31.79; 29.10, 29.08, 26.73; 22.25; 21.45 ppm; MS-CI (100 eV): m/z (%): 386 (86.4) $[M+2]^+$, 384 (89.6) $[M]^+$, 348 (60.0), 278 (75.5), 252 (65.5), 251 (62.8), 250 (100), 249 (77.7), 248 (59.3), 208 (32.7), 194 (53.4), 180 (41.4), 166 (33.8).

Cleaning process of Si ATR (attenuated total reflection) crystal for monolayer coating: The silicon ATR crystal obtained from Korth GmbH, Berlin (paralleliped with an angle of 45°, 72 mm × 12 mm × 6 mm, 12 reflections) was consecutively sonicated in acetone, deionized water, and isopropanol. It was then blow-dried with N_2 and exposed to an oxygen plasma in a plasma cleaner (Tepla AG, Germany, 100-E) at 100 W, 0.5 mbar, 60 min on each side. The crystal was then immersed in deionized water for 0.5 h and blow-dried with N_2.

Preparation of bromo-terminated SAMs (method 1): A freshly cleaned silicon ATR crystal was immersed in a solution of BUTS (3 mL, 1 mM) in toluene (dried with Al_2O_3, neutral) for 16 h at 25 °C. The crystal was then washed with dry toluene and sonicated with acetone and THF.

Preparation of amino-terminated SAMs:[4] The amino-terminated SAMs were prepared from bromo-terminated SAMs by adopting the procedure described in reference [4]. Briefly, the bromo-terminated substrate was immersed in a solution of sodium azide (3 mL, 10 mM) in DMF at room temperature for 24 h or 72 h. The substrate was then washed with DMF and sonicated (acetone, Millipore H_2O, and THF). The azide-terminated SAMs were further reduced with a saturated solution of $LiAlH_4$ in ether for 1 h. The substrate was copiously rinsed with THF, Millipore H_2O, 10% HCl, and Millipore H_2O, and then immersed in a 5 mM NaOH solution for 1 min and rinsed with Millipore H_2O. The surface transformations were characterized and controlled with IR spectroscopy and contact angle measurements. The nucleophilic displacement of bromo groups on surface by the azide groups gave to a strong IR absorption at 2098 cm^{-1}. This peak disappeared when the azide groups were reduced to amino groups by $LiAlH_4$. The conversions were also confirmed by the contact angle measurement. The advancing contact angles alter from 90° (bromo-terminated surface) to 85° (azide-terminated) and finally to 64° (amino-terminated one), in accordance with reference [4].

Reaction of amino-terminated SAMs with hetero-crosslinker sulfosuccinimidyl-4-(*N*-maleimidomethyl)cyclohexane-1-carboxylate (SSMCC):[20] The obtained amino-terminated SAMs were reacted with SSMCC (100 μL, 1.5 mM) in triethanolamine buffer solution (addition of NaOH/HCl to adjust to pH 7) at 25 °C for 16 h, and then washed with H_2O, and sonicated with acetone, THF.

Preparation of maleimido monolayers from bromo-SAMs (method 2): K_2CO_3 (3 g) and DMF (10 mL) were added to a flask and vigorously stirred for 16 h. The undissolved excess K_2CO_3 was filtered off. PM (10 mM) was dissolved in saturated K_2CO_3/DMF solution (3 mL), and allowed to react with the obtained bromo-SAMs at 70 °C for 16 h. The ATR crystal was then intensively washed with DMF, sonicated with acetone and THF, and blow-dried with N_2. The ATR crystal was heated in an oven at 170 °C for 2 h to transform the protected maleimido-terminated SAMs into the maleimido-terminated analogue.

Preparation of maleimido SAMs from H-terminated silicon (method 3): The silicon ATR crystal was sonicated with acetone, deionized water, and isopropanol, respectively, and then blow-dried with N_2. In a plasma cleaner, a hydrogen plasma (Tepla AG, Germany, 100-E) at 100 W, 0.5 mbar was applied to each side of the ATR crystal for 60 min. The H-terminated silicon ATR after the measurement of IR background was immediately immersed in a solution of MU (3 mL, 100 mM) in mesitylene at 175 °C for 2 h under an argon atmosphere. 'The ATR was then washed with mesitylene and sonicated with acetone, THF.

Preparation of maleimido-terminated SAMs via MUTS (method 4) and mixed monolayers: Similarly to the formation of bromo-terminated SAMs, the freshly O_2-plasma-cleaned silicon ATR crystal was immersed in a solution of MUTS (3 mL, 1 mM) in toluene for 16 h at 25 °C. The crystal was then washed with dry toluene and sonicated with acetone, THF.

Mixed monolayers were prepared with the solution composed of MUTS and DTS in dry toluene. The molar MUTS:DTS mixing ratios were 1:0, 2:1, 1:2, and 0:1, while the total molar amount of MUTS and DTS were 1 mM.

Reaction of maleimido-terminated SAMs with decylthiol and octadecylthiol: Maleimido-terminated SAMs obtained with method 4 were immersed in a solution of alkylthiol (3 mL, 100 mM decylthiol and octadecylthiol) in EtOH at 50 °C overnight. The sample was then washed with EtOH and sonicated with acetone, THF.

Reaction of maleimido-terminated SAMs with 5-cyanoindole (CI): Maleimido-terminated SAMs obtained with method 4 were immersed in a solution of 5-cyanoindole (3 mL, 100 mM) in AcOH and refluxed under an N_2 atmosphere for 96 h. The sample was then washed with AcOH and sonicated with acetone, THF.

Reaction of maleimido-terminated SAMs with 2-cyano-thioacetamide (CTA): Maleimido-terminated SAMs obtained with method 4 were immersed in a solution of 2-cyano-thioacetamide (3 mL, 100 mM) in EtOH under refluxing conditions in the presence of a catalytic amount of triethylamine (0.05 mL) for 2 h. The sample was then washed with EtOH and sonicated with acetone and THF.

Reaction of maleimido-terminated SAMs with aminocapronitrile (ACN): Maleimido-terminated SAMs obtained with method 4 were immersed in a solution of aminocapronitrile (3 mL, 100 mM) in EtOH at 50 °C overnight. The sample was then washed with EtOH and sonicated with acetone, THF.

Immobilization of DNA oligonucleotides on maleimidio-terminated SAMs: Oligonucleotides with a thiol-modification at the 3′-end were obtained from MWG (Germany). The oligonucleotides are 31 nt in length with a 15 mer dT spacer and a specific 16 mer sequence, that is, 3′-HSC6-T15-AA-CGA-TCG-AGC-TGC-AA-5′. The oligonucleotides were used immediately after delivery by the company. The silicon wafer (5 mm × 5 mm), modified with maleimido-terminated SAMs, was placed face-up (polished side) in a chamber saturated with water vapor. A DNA solution (≈100 μL of 5 μM) in an aqueous buffer (NaH_2PO_4 10 mM, NaCl 1 M, pH 7) was added onto the surface. After 16 h, the wafer was rinsed with a copious amount of the buffer solution, immersed in distilled water for half an hour, and blow-dried with N_2.

IR spectroscopy of the monolayers: FT-IR measurements of the monolayers were recorded with a Bruker IFS 66 V spectrophotometer with a DTGS detector. All measurements were made until the sample chamber was evacuated to 4×10^{-4} mbar. Spectra were recorded with 4 cm^{-1} resolution, 1000–3000 scans, and application of a Blackman–Harris 3-term apodization function in the Fourier transformation. Reference spectra were recorded with freshly cleaned ATR spectra. The absorption spectra of the corresponding functionalized SAMs in the process of formation, mixed monolayers formation, and reactivity verification were obtained by subtracting the reference spectrum from the absorbance spectrum of the coated substrate.

X-ray photoelectron spectroscopy: X-ray photoelectron spectra were recorded with a PHI 5800 ESCA System (Physical Electronics) and monochromatized $Al_{K\alpha}$ radiation (1486.6 eV) as the excitation source and a hemispherical analyzer with 150 mm radius. The takeoff angle was set to 45°. The silicon wafer samples with a size of 1 cm × 0.5 cm were mounted on sample stubs with conductive carbon tape. Spectra were recorded with a pass energy of 187.85 eV (survey scans) or 29.35 eV (high-resolution scans). Atomic concentrations of elements within the electron escape depth were determined by evaluating the integral intensities of N 1s, Br 3d, Si 2p, O 1s and C 1s signals and taking into account the tabulated atomic sensitivity factors and the instrument transmission.[32] The spectra were referenced by setting the peak of the saturated hydrocarbon C 1s to 284.5 eV to compensate for residual charging effects.

Ellipsometry: The thicknesses of the prepared monolayers from methods 1–4 were obtained with a spectroscopic ellipsometer MM301 (OMT, Germany). The measurements were performed with an incident angle of 70° and a wavelength range of 350–900 nm. For each sample, 3–6 measurements were analyzed with the proprietary software of OMT. The refractive indices of the organic monolayers and the SiO_2 layers were both assumed to be 1.45.

Atomic force microscopy: AFM was carried out with a Digital Instruments Multimode Nanoscope IIIa instrument operating in tapping mode. The tips used were Olympus (DI NanoSensors) Tapping Mode Etched $n(+)$-silicon probes (force constant: 21–78 $N m^{-1}$; resonant frequency: 250–390 kHz). Image analysis was performed offline with roughness and section commands with the Nanoscope program for AFMs.

Contact angle measurements: Water contact angles were measured by means of the sessile drop method on a goniometer (Krüss DSA10) at 25 °C and ambient humidity. Advancing and receding contact angles were measured on both sides of the ATR crystals. At least six measurements were performed on each side. Data in the Figure represent the average of these measurements.

Acknowledgements

We thank M. Möller, B. Rieger, K. Landfester (University of Ulm), H. Auweter, and R. Iden (BASF-Aktiengesellschaft) for supporting these investigations, as well as J. Demeter for providing the aminocapronitrile. This work was financially supported by the Deutsche Forschungsgemeinschaft through the Research Training Group 328.

[1] a) G. L. Gaines, Jr., *Insoluble Monolayers at Liquid-Gas Interfaces*, Interscience, New York, **1966**; b) G. Roberts, *Langmuir-Blodgett Films*, Plenum Press, New York, **1990**; c) A. Ulman, *An Introduction to Ultrathin Organic Films*, Academic Press, San Diego, **1991**.
[2] a) C. D. Bain, E. B. Troughton, Y.-T. Tao, J. Evall, G. M. Whitesides, R. G. Nuzzo, *J. Am. Chem. Soc.* **1989**, *111*, 321–335; b) M. Grunze, *Phys. Scr.* **1993**, *T49B*, 711–717; c) L. A. Wenzler, G. L. Moyes, G. N. Raikar, R. L. Hansen, J. M. Harris, T. P. Beebe, L. L. Wood, S. S. Saavedra, *Langmuir* **1997**, *13*, 3761–3768.
[3] A. Ulman, *Chem. Rev.* **1996**, *96*, 1533–1554.
[4] N. Balachander, C. N. Sukenik, *Langmuir* **1990**, *6*, 1621–1627.
[5] P. A. Lewis, R. K. Smith, K. F. Kelly, L. A. Bumm, S. M. Reed, R. S. Clegg, J. D. Gunderson, J. E. Hutchison, P. S. Weiss, *J. Phys. Chem. B* **2001**, *105*, 10630–10636.
[6] Y. T. Tao, C. Y. Huang, D. R. Chiou, L. J. Chen, *Langmuir* **2002**, *18*, 8400–8406.
[7] R. Arnold, W. Azzam, A. Terfort, C. Wöll, *Langmuir* **2002**, *18*, 3980–3992.
[8] M.-T. Lee, G. S. Ferguson, *Langmuir* **2001**, *17*, 762–767.
[9] G. E. Fryxell, P. C. Rieke, L. L. Wood, M. H. Engelhard, R. E. Williford, G. L. Graff, A. A. Campbell, R. J. Wiacek, L. Lee, A. Halverson, *Langmuir* **1996**, *12*, 5064–5075.
[10] A. B. Sieval, R. Linke, G. Heij, G. Meijer, H. Zuilhof, E. J. R. Sudhölter, *Langmuir* **2001**, *17*, 7554–7559.
[11] N. Tillman, A. Ulman, T. L. Penner, *Langmuir* **1989**, *5*, 101–111.
[12] S. R. Wasserman, Y. T. Tao, G. M. Whitesides, *Langmuir* **1989**, *5*, 1074–1087.
[13] L. Netzer, R. Iscovichi, J. Sagiv, *Thin Solid Films* **1983**, *99*, 235–241.
[14] B. T. Houseman, E. S. Gawalt, M. Mrksich, *Langmuir* **2003**, *19*, 1522–1531.
[15] X. Wang, D. Zhou, T. Rayment, C. Abell, *Chem. Commun.* **2003**, *4*, 474–475.
[16] C. R. Yonzon, E. Jeoung, S. Zou, G. C. Schatz, M. Mrksich, R. P. van Duyne, *J. Am. Chem. Soc.* **2004**, *126*, 12669–12676.
[17] D.-H. Min, M. Mrksich, *Curr. Opin. Chem. Biol.* **2004**, *8*, 554–558.
[18] S. J. Oh, S. J. Cho, C. O. Kim, J. W. Park, *Langmuir* **2002**, *18*, 1764–1769.
[19] S. J. Xiao, M. Textor, N. D. Spender, H. Sigrist, *Langmuir* **1998**, *14*, 5507–5516.
[20] T. Strother, R. J. Hamers, L. M. Smith, *Nucleic Acids Res.* **2000**, *28*, 3535–3541.
[21] R. C. Clevenger, K. D. Turnbull, *Synth. React. Inorg. Met.-Org. Chem. Synth. Comm.* **2000**, *30*, 1379–1388.
[22] H. Kwart, I. Burchuk, *J. Am. Chem. Soc.* **1952**, *74*, 3094–3097.
[23] The reverse Diels–Alder reaction is thought to be a very useful method for the preparation of *N*-substituted maleimides that can not be obtained by direct dehydration of maleimic acids owing to the formation of the corresponding isomaleimides. See, M. Narita, T. Teramoto, M. Okawara, *Bulleid Meml. Lect. Bulletin Chem. Soc. Japan* **1971**, *44*, 1084–1089.
[24] S. F. Parker, *Spectrochim. Acta Part A* **1995**, *51*, 2067–2072.
[25] Y. Wang, M. Lieberman, *Langmuir* **2003**, *19*, 1159–1167.
[26] S. Chen, L. Li, C. L. Boozer, S. Jiang, *Langmuir* **2000**, *16*, 9287–9293.
[27] R. G. Snyder, H. L. Strauss, C. A. Elliger, *J. Phys. Chem.* **1982**, *86*, 5145–5150.
[28] A. B. Sieval, R. Linke, G. Heij, G. Meijer, H. Zuilhof, E. J. R. Sudhölter, *Langmuir* **2001**, *17*, 7554–7559.
[29] H. Hoffmann, U. Mayer, A. Krischanitz, *Langmuir* **1995**, *11*, 1304–1312.
[30] Numbers in parenthesis are the relative areas obtained by fitting the peak with Gauss–Lorentz peaks, as indicated in Figure 6a.
[31] K. R. Finnie, R. Haasch, R. G. Nuzzo, *Langmuir* **2000**, *16*, 6968–6976.
[32] J. F. Moulder, W. F. Stickle, P. E. Sobol, K. D. Bomben, *Handbook of X-ray Photoelectron Spectroscopy*, Eden Prairie, **1995**, Physical Electronics, Inc..
[33] J. P. Folkers, P. E. Laibinis, G. M. Whitesides, *Langmuir* **1992**, *8*, 1330–1341.
[34] J. E. Macor, D. H. Blank, K. Ryan, R. J. Post, *Synthesis* **1997**, 443–449.
[35] F. M. Abdel-Galil, M. M. Sallam, S. M. Sherif, M. H. Elnagdi, *Heterocycles* **1986**, *24*, 3341–3346.
[36] C. Hulubei, V. Cozan, M. Bruma, *High Performance Polymers*, **2004**, *16*, 405–418.
[37] C. S. Marvel, W. E. Garrison, *J. Am. Chem. Soc.* **1959**, *81*, 4737–4744.
[38] M. A. Apfel, H. Finkelmann, G. M. Janini, R. J. Laub, B. H. Lühmann, A. Price, W. L. Roberts, T. J. Shaw, C. A. Smith, *Anal. Chem.* **1985**, *57*, 651–658.

Received: September 2, 2004
Revised: January 24, 2005
Published online: April 21, 2005